QuadCam - a quadruple polarimetric camera for space situational awareness

Jovan Skuljan
Defence Technology Agency, Auckland, New Zealand

ABSTRACT

A specialised quadruple polarimetric camera for space situational awareness, QuadCam, has been built at the Defence Technology Agency (DTA), New Zealand, as part of collaboration with the Defence Science and Technology Laboratory (Dstl), United Kingdom. The design was based on a similar system originally developed at Dstl, with some significant modifications for improved performance. The system is made up of four identical CCD cameras looking in the same direction, but in a different plane of polarisation at 0, 45, 90 and 135 degrees with respect to the reference plane. A standard set of Stokes parameters can be derived from the four images in order to describe the state of polarisation of an object captured in the field of view.

The modified design of the DTA QuadCam makes use of four small Raspberry Pi computers, so that each camera is controlled by its own computer in order to speed up the readout process and ensure that the four individual frames are taken simultaneously (to within 100-200 microseconds). In addition, a new firmware was requested from the camera manufacturer so that an output signal is generated to indicate the state of the camera shutter. A specialised GPS unit (also developed at DTA) is then used to monitor the shutter signals from the four cameras and record the actual time of exposure to an accuracy of about 100 microseconds. This makes the system well suited for the observation of fast-moving objects in the low Earth orbit (LEO).

The QuadCam is currently mounted on a Paramount MEII robotic telescope mount at the newly built DTA space situational awareness observatory located on Whangaparaoa Peninsula near Auckland, New Zealand. The system will be used for tracking satellites in low Earth orbit and geostationary belt as well. The performance of the camera has been evaluated and a series of test images have been collected in order to derive the polarimetric signatures for selected satellites.

1. INTRODUCTION

Over the past couple of years, there has been a steady increase in the space situational awareness (SSA) capability within the New Zealand Defence Force (NZDF). This came mainly as a result of close collaboration between the Defence Technology Agency (DTA) and the Defence Science and Technology Laboratory (Dstl), United Kingdom. After the initial success of wide-field observations and astrometric position measurements of satellites in low Earth orbit in 2015, using some standard off-the-shelf electro-optics equipment [1], a decision was made to extend this capability to include photometry and polarimetry of orbiting bodies, as additional tools for characterisation of satellites in situations where they cannot be resolved using high-resolution imaging. Some upgrade to the existing equipment and observing facilities was required in order to achieve this goal. Unlike the previous experience with wide-field imaging, where the satellite trails were recorded against a fixed stellar background by keeping the cameras static (or moving slowly at the sidereal rate), the photometric and polarimetric characterisation of satellites can be efficiently done only if the camera follows the satellite in its orbit, using a fast tracking mount. This also requires a permanent observing facility, as the telescope mount needs to be accurately aligned with the Earth's rotation axis in order to be able to find a satellite in the sky and follow it during the entire pass. A new DTA SSA observatory was completed early this year in order to support this type of observation and data collection.

The main piece of equipment used in this project is a specialised polarimetric camera built at DTA, based on a polarimetric imager originally developed at Dstl and used by Grant Privett [2] to successfully detect aircraft debris at sea. The original UK design was somewhat modified when the NZ unit was built, in order to improve the performance, keeping the main design features unchanged.

There are only a limited number of reports of polarimetric observations of satellites in the literature [3]. While measuring the polarimetric signatures of orbiting bodies can be a relatively straightforward task, the interpretation of data requires additional research and theoretical modelling of polarisation of light reflected from a satellite, which

involves a number of parameters such as the satellite shape and size, properties of the materials reflecting the light, orientation in space, viewing geometry and instrumental effects. At this stage we are going to report some measurements obtained with the new DTA polarimetric camera, concentrating mainly on the camera performance and pointing out only some basic features observed in the polarimetric signatures.

2. OBSERVING EQUIPMENT

The main piece of equipment used in this project is the DTA quadruple polarimetric camera, or QuadCam, recently constructed for polarimetric SSA observations (Fig. 1). The system consists of four identical CCD cameras looking in the same direction, but in a different polarisation plane. The individual cameras are Starlight Xpress SuperStar auto-guiders, based on the Sony ICX205AL monochrome CCD detector with a resolution of 1392 × 1040 and pixel size of 4.65μm. These cameras operate at ambient temperature, which limits the exposure time to a maximum of a few seconds, to avoid any excessive thermal noise. Each SuperStar camera is fitted with a Nikon AF NIKKOR 50 mm f/1.8D lens, which provides manual aperture and focus controls. A standard UV/IR blocking filter is added to limit the spectral range to visible light. Finally, a linear polariser is used to select only one plane of polarisation. The four cameras are arranged in an 80 mm × 80 mm square pattern, with cameras 1 and 2 at the top and cameras 3 and 4 at the bottom. Each SuperStar camera is controlled by a Raspberry Pi computer (camera server) under Linux. The control PC communicates with the four camera servers over the network. The control software was developed in Delphi as a multi-thread application, to minimise any delay between the end of exposure and image readout.

The angle of polarisation for each camera is shown schematically in the right panel of Fig. 1. Looking into the camera from the front, the polarisation angle increases in the clockwise direction as the camera number increases. However, when looking into the corresponding CCD images, the polarisation angle increases in the usual, anti-clockwise direction. It should be noted that although the angle of 0° appears to correspond to the horizontal plane when the camera is placed on a bench, it becomes the plane of a declination circle in the sky when the camera is attached to the telescope mount. In this arrangement, the polarisation angle of 90° represents the equatorial plane.

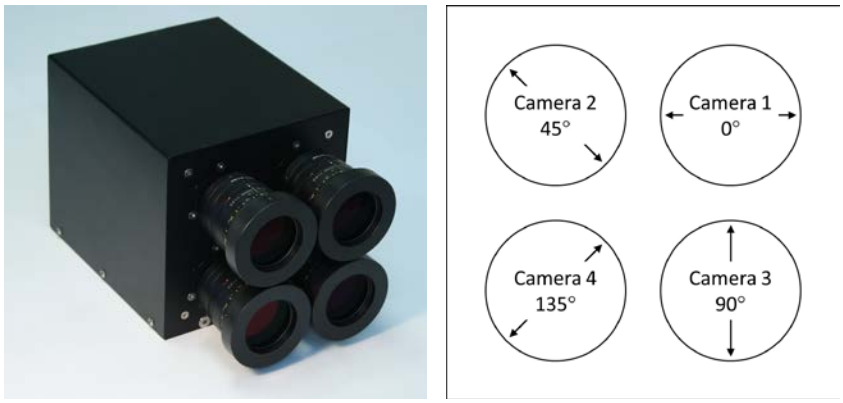

Fig 1. DTA quadruple polarimetric camera (left) and the arrangement of polarisation planes (right).

A special GPS unit is used with the DTA polarimetric camera to accurately record the start and finish of every exposure. The device was designed and manufactured at DTA by Theo Zlatanov and is capable of recording the time down to microsecond accuracy, using a U-blox LEA 6-T GPS receiver (Fig. 2). In addition to the standard NMEA (National Marine Electronics Association) message and a 1 Hz pulse, the receiver also provides a high frequency 1 MHz pulse for increased time resolution. At the same time, a separate on-board microcontroller (PIC32) is programmed to constantly monitor the signal levels on four external inputs (provided by the four CCD cameras), looking for a falling, or rising edge. When an edge occurs, the time is recorded using the high-resolution pulse from the GPS receiver and the information is saved onto a memory card. While the cameras are inactive, the shutter signals are high. As soon as an exposure is started on one of the cameras, the corresponding signal falls to zero and stays low during the exposure. The signal becomes high again when the exposure is finished. The SuperStar auto-guiders do not normally provide a shutter signal of this kind, but a special firmware was obtained from the manufacturer, Starlight Xpress, to enable this feature. The shutter signal is supplied on one of the pins on the auto-guiding port at the back of the camera.

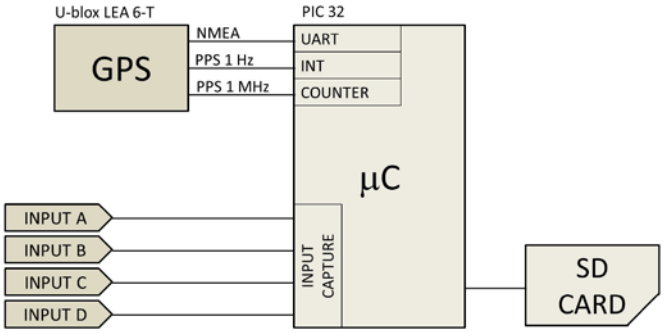

Fig. 2. GPS timing unit used with the DTA QuadCam.

Although the GPS timing unit has an internal precision of 1 µs, the actual start and finish of an exposure can only be determined to an accuracy of 100 – 200 µs, due to the intrinsic latencies involved during the generation of the shutter signal inside the camera and the fact that a signal edge always has a finite slope (i.e. is not perfectly sharp). However, the overall accuracy remains well below 1ms, which is ideal for observations of satellites in low Earth orbit. We should also mention that in this particular application, the accuracy on the exposure timing has little effect on the photometry, since a typical exposure with this system takes several seconds, but it is essential for astrometry, when the position of a satellite is measured with reference to the background stars, or star trails. The satellite astrometry is not presented in this paper, but is a standard part of the SSA image analysis process.

DTA now operates a small SSA observatory located at the tip of Whangaparaoa Peninsula, at a latitude of 36° 36′ 8.5″ S and longitude of 174° 50′ 5.6″ E, at about one hour's drive north of Auckland. The observatory has a 3-metre fibreglass dome and is equipped with a Paramount MEII robotic telescope mount and a Celestron EdgeHD 11-inch telescope. The polarimetric camera is mounted side-by-side with the telescope. Both the telescope mount and the dome are controlled from a central computer using TheSkyX control software. At this stage, physical presence of an observer is required when the equipment is being used, but this will change in the future, when the facility becomes fully automated.

3. POLARIZATION OF LIGHT

Any state of polarisation of light can be described using a set of four Stokes parameters S_0, S_1, S_2 and S_3 [4, 5]. The first parameter, S_0, represents the total flux, while the remaining three describe the state of polarisation. We will consider here only the parameters S_1 and S_2, which are related to linear polarisation. The last Stokes parameter, S_3, describes the circular polarisation and will be ignored.

When the intensity of light is measured for the same source in four different planes of polarisation, positioned at 0°, 45°, 90° and 135° with respect to a fixed reference plane, the Stokes parameters can be calculated from:

$$S_0 = I_{0^\circ} + I_{90^\circ} = I_{45^\circ} + I_{135^\circ}$$
$$S_1 = I_{0^\circ} - I_{90^\circ}$$
$$S_2 = I_{45^\circ} - I_{135^\circ}$$

However, it is more convenient to use the normalized expressions for S_1 and S_2:

$$s_1 = 2\,S_1/S_0$$
$$s_2 = 2\,S_2/S_0$$

The degree of linear polarisation (P) and angle of polarisation (θ) are then defined as:

$$P = \sqrt{{s_1}^2 + {s_2}^2}, \qquad \theta = \frac{1}{2}\tan^{-1}\frac{s_2}{s_1}$$

4. PHOTOMETRIC CALIBRATION

In order to be able to measure the brightness of a satellite, the system must be properly calibrated using a set of known stars. A typical calibration image is shown in Fig. 3. The field is centred at a right ascension of about $\alpha_0 = 16^h$ and declination of $\delta_0 = -41°$, in the vicinity of the 5-magnitude star HIP 78323 and also including the bright star η Lupi (magnitude 3.4) at the northern edge of the frame. The exposure time is 5 seconds. An average of six frames was computed in order to reduce the noise. The longer (horizontal) axis of the frame is aligned with the north-south direction, with the south celestial pole to the left and the celestial equator to the right. The pixel scale is about 18.5 arc seconds per pixels, and the total field of view is 7.2° × 5.4°. In the right-hand panel, a zoomed-in region of 200 × 200 pixels is shown to illustrate the star detection limit in the presence of the thermal noise. A number of faint stars are labelled, using a standard way of marking the stellar magnitudes in astronomical images, by omitting the decimal point (which, otherwise, might be confused with faint stars). The star detection limit is estimated to be around magnitude 10, but the flux measurement at this level can become very difficult due to the noise.

The photometric calibration was performed using a number of stars covering a range of magnitudes between 10 and 3.4. We are ignoring the fact that our images were not taken using a standard set of photometric filters. This might increase the uncertainty of the calibration, but will still give us a good indication of the visual magnitude obtained from our measurements. Standard aperture photometry was used to estimate the total flux received from a star. This was done by placing a circular aperture of a fixed radius of four pixels centred at the star and summing up the pixel values inside the circle. An additional ring of four pixels around the circular aperture was used to estimate the background level, by calculating the median value of all pixels inside the ring. The median background was subtracted from every pixel value inside the photometric aperture before the total flux was computed.

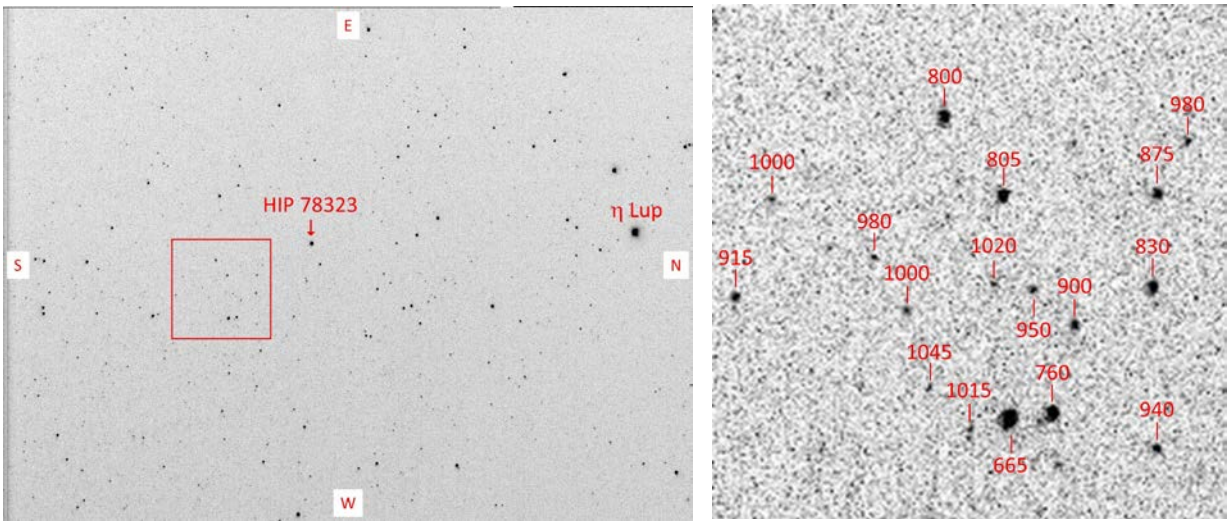

Fig. 3. Calibration frame (left) and a zoomed-in region (right). The visual magnitudes are marked with the decimal point omitted.

The photometric calibration is presented in Fig. 4, where the stellar magnitude is plotted against the measured total flux on a logarithmic scale. A satisfactory linear fit was obtained. The measured slope of 2.67 is reasonably close to the theoretical value of 2.5 (as obtained from Pogson's formula [6]).

The photometric calibration described above was performed only for our reference camera 1. It was noted that different cameras consistently give slightly different response (up to about 20 per cent in some cases), both in the total amount of dark counts (i.e. when the aperture is closed) and also when detecting photons from the same unpolarised source. These differences were measured separately by analysing the images of the same stellar field taken with different cameras. As a result of this analysis, a set of correction coefficients was produced for the conversion between the fluxes obtained with different cameras. These corrections were applied to every satellite measurement before calculating the total flux and Stokes parameters.

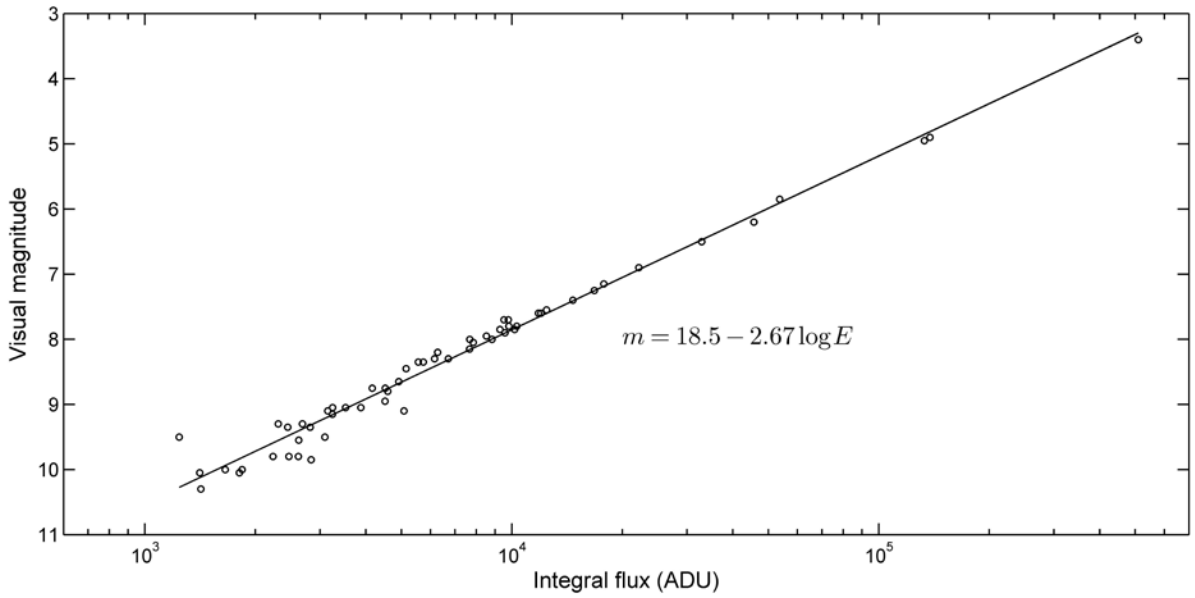

Fig. 4. Photometric calibration

5. SATELLITE OBSERVATIONS

A number of satellites in low Earth orbit (LEO) were observed over three nights during August 2017 in order to test the performance of the DTA polarimetric camera. Suitable targets were initially selected from Heavens-Above [7], and the list was then combined with the current version of the NORAD catalogue, obtained from CelesTrak [8], while the latest TLE orbital data were downloaded from Space-Track [9]. Eight satellites were selected to be included in this paper, as shown in Table 1. The satellite names were taken from Heavens-Above, while the NORAD catalogue numbers and COSPAR international designations were derived from the TLE orbital elements. The observation date shown in Table 1 corresponds to the middle point on the observed trajectory. Normally, this should correspond to the highest point in the sky, unless the satellite was obstructed at either end of the pass by clouds, or the Earth's shadow.

Table 1. Satellite observations

Satellite name	*NORAD*	*COSPAR*	*Observation date (UTC)*
Cosmos 1455	14032	83037A	2017-Aug-04 06:46
Cosmos 1027 Rocket	10992	78074B	2017-Aug-04 07:09
Cosmos 2369	26069	00006A	2017-Aug-04 08:12
Meteor 1-11 Rocket	5918	72022B	2017-Aug-22 07:52
Meteor 2-1	8026	75064A	2017-Aug-23 07:31
Cosmos 2219 Rocket	22220	92076B	2017-Aug-23 07:49
Cosmos 2279	23092	94024A	2017-Aug-23 08:00
Cosmos 2237 Rocket	22566	93016B	2017-Aug-23 08:34

A typical satellite image is shown in Fig. 5. The satellite appears as a reasonably well defined point source close to the middle of the frame, while stars are shown as streaks, whose length depends on the tracking speed and exposure duration. It is possible to use the stellar traces to perform astrometric calibration and obtain the position of the satellite at any time during the exposure, although this was not part of the data analysis presented in this paper. The main measurement goal was to obtain the total flux received from the satellite, using aperture photometry in the

same way as in our calibration images described above. We use our specialised data analysis tool called StarView [1], which was recently upgraded to enable the analysis of QuadCam images. Some additional analysis tasks were performed in Matlab.

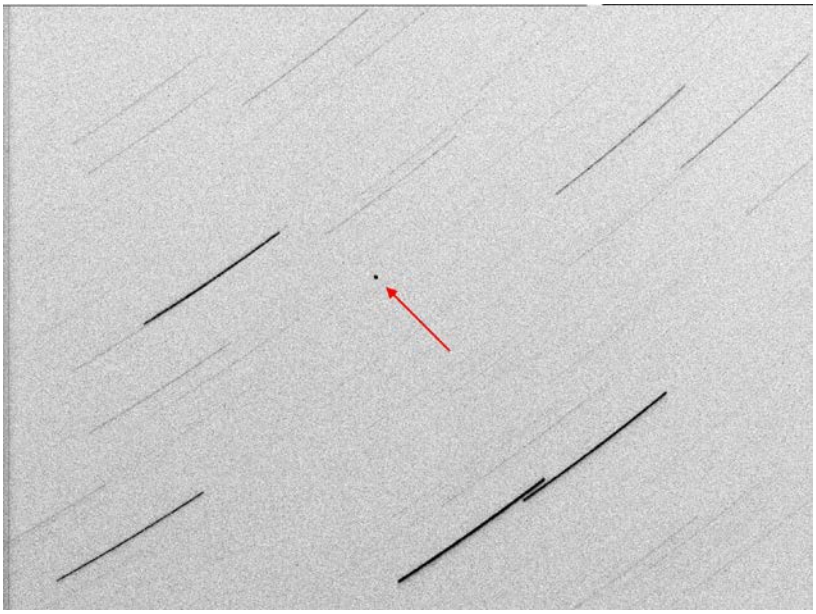

Fig. 5. Cosmos 1027 Rocket (NORAD 10992) exposed for 5 seconds on 4 Aug 2017 at 7:09 UTC

The results of the photometric and polarimetric measurements are shown in figures 6 – 13. Each figure consists of four panels, with the top two panels displaying the total flux (visual magnitude) and the normalised Stokes parameters s_1 and s_2. The bottom two graphs show the degree and angle of polarisation. No attempt has been made at this stage to produce complete interpretation of the polarimetric signatures recorded during this experiment, but such analysis might be included in the future. Some general comments and observations about the recorded signatures are summarised below:

- It is evident that the polarimetric signatures provide additional information which otherwise cannot be derived from the light curve alone. A good example is Cosmos 2369 (Fig. 8). While the light curve is mainly featureless, the Stokes parameters reveal a varying degree of polarisation and a slowly rotating plane of polarisation. This gradual change in polarisation is probably a result of slowly varying geometry. The diagrams provide no evidence of any unusual behaviour.
- Occasionally, a sudden flip in the polarisation plane is observed, as a discontinuity in the polarisation angle, for example in Cosmos 1027 Rocket (Fig. 7). The flip in this case is about 90° and it occurs while the satellite is passing through a point of zero polarisation, at about 7:08 UTC. The Stokes parameters s_1 and s_2 both change their sign from negative to positive during this transition.
- Some satellites, like Cosmos 1455 (Fig. 6) display plenty of activity in the total flux, with occasional sudden glints, followed by deeper dimming (with a total change in brightness of 1 – 2 magnitudes in this case), while the polarisation curves stay virtually unaffected. A 90° flip in the polarisation plane is also observed when the Stokes parameters change their sign at about 6:48 UTC.
- An interesting case of a possibly tumbling rocket body is displayed by Cosmos 2219 Rocket (Fig. 11). The total flux shows almost periodic variations with a period of a few seconds and an amplitude of 0.5 – 1 magnitude, up to the point of maximum brightness. At the same time, the linear polarisation remains very low and without any obvious change (there is some noticeable noise in the polarisation angle due to the fact that the degree of polarisation is close to zero, see comment below).
- For most satellites, the degree of linear polarisation remains relatively low (below 20% in most cases). The measurement of the polarisation angle can become very uncertain when the degree of polarisation is low (i.e. when both s_1 and s_2 are close to zero). Such measurements are usually discarded.

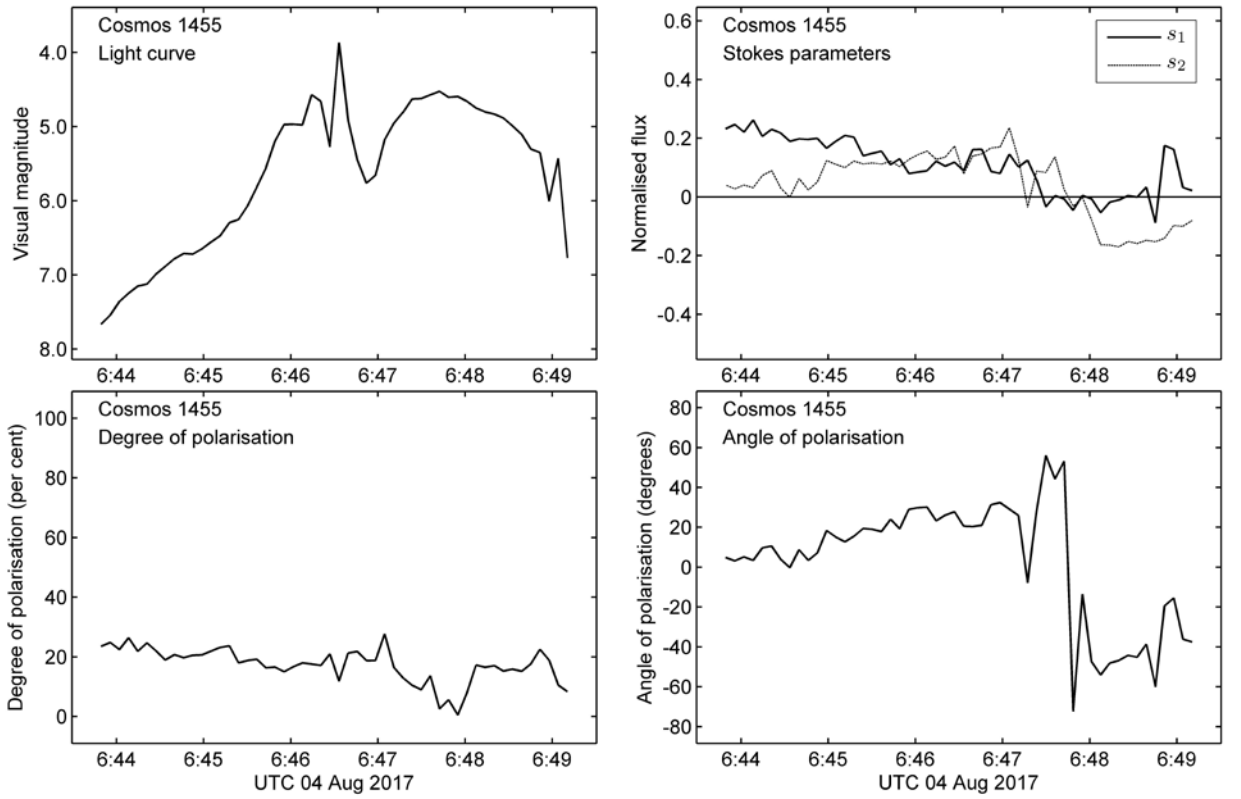

Fig. 6. Light curve and polarimetric signature of Cosmos 1455 (NORAD 14032).

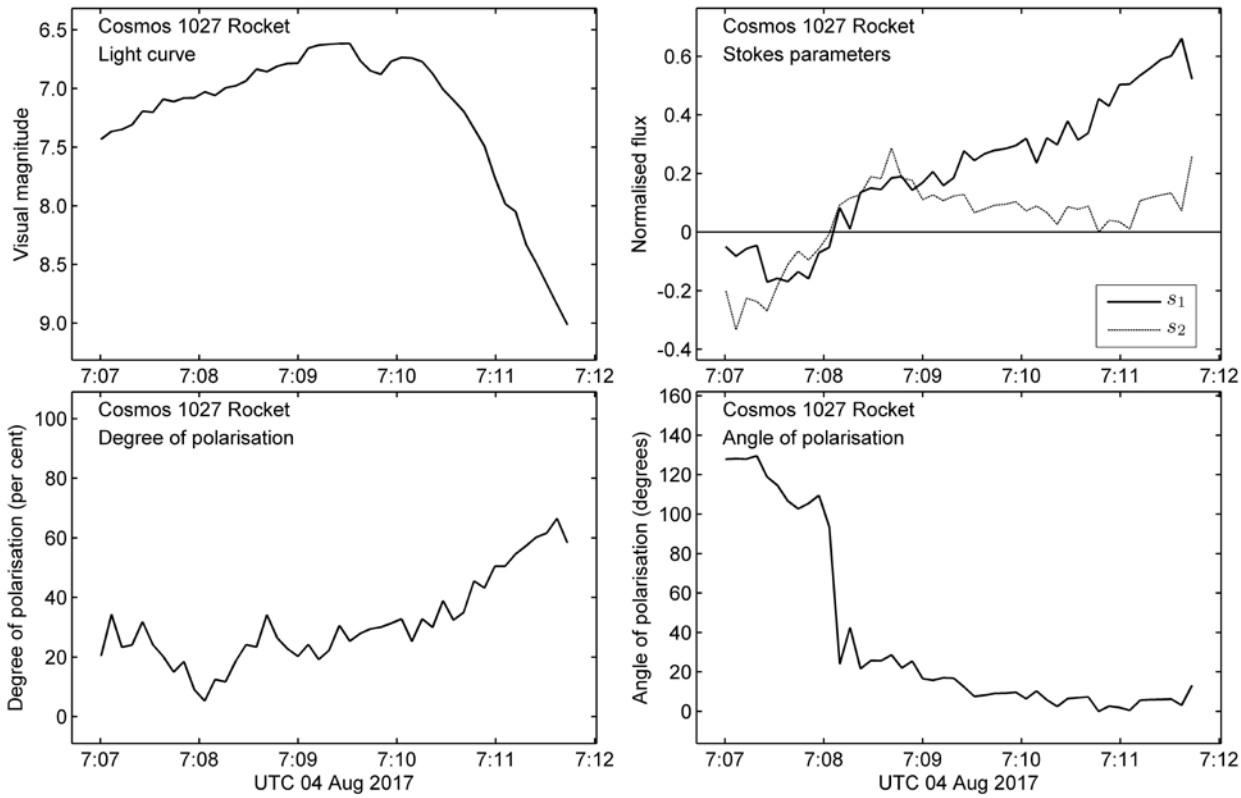

Fig. 7. Light curve and polarimetric signature of Cosmos 1027 Rocket (NORAD 10992).

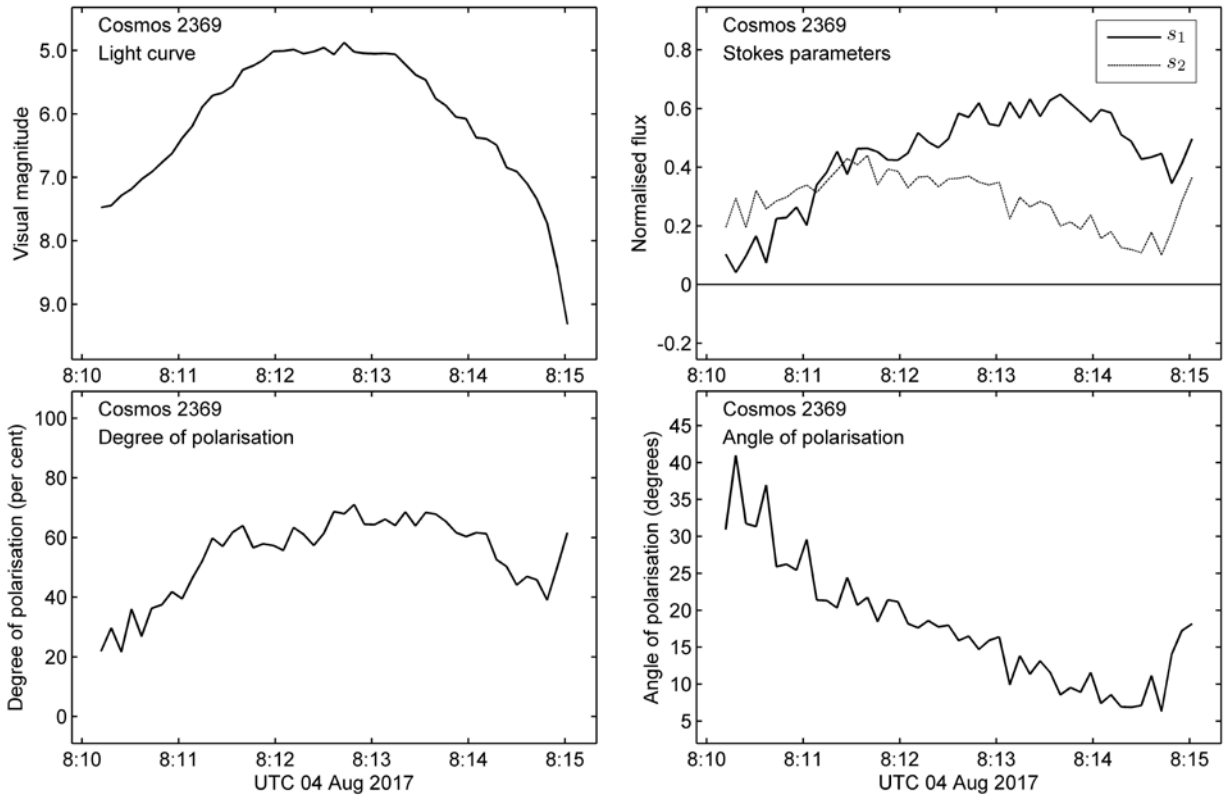

Fig. 8. Light curve and polarimetric signature of Cosmos 2369 (NORAD 26069).

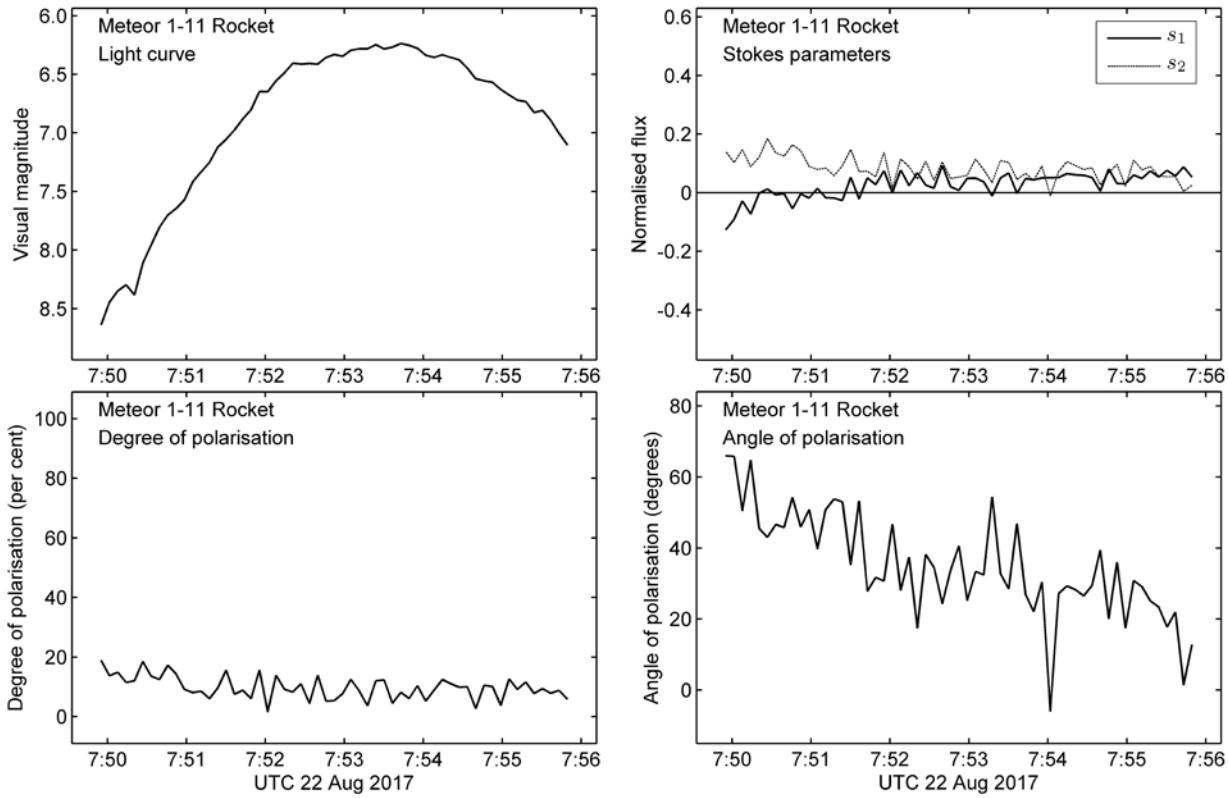

Fig. 9. Light curve and polarimetric signature of Meteor 1-11 Rocket (NORAD 5918).

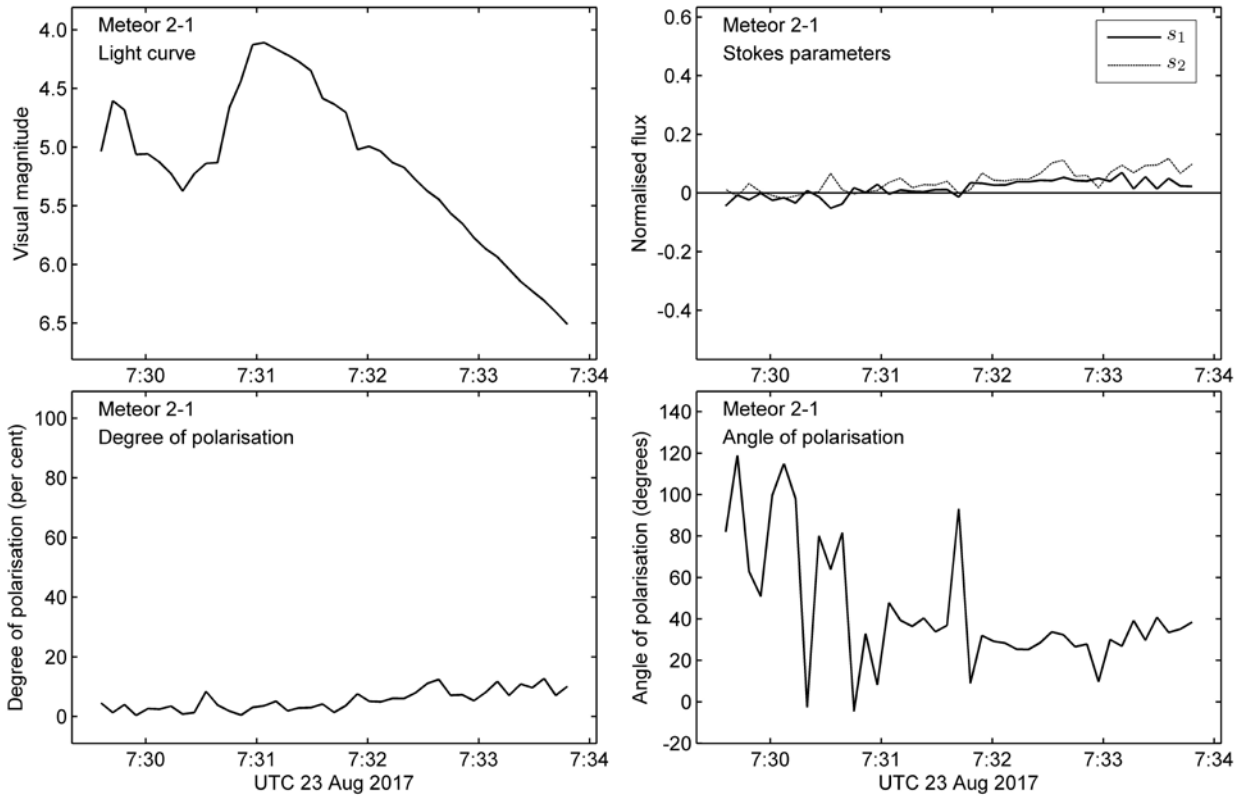

Fig. 10. Light curve and polarimetric signature of Meteor 2-1 (NORAD 8026).

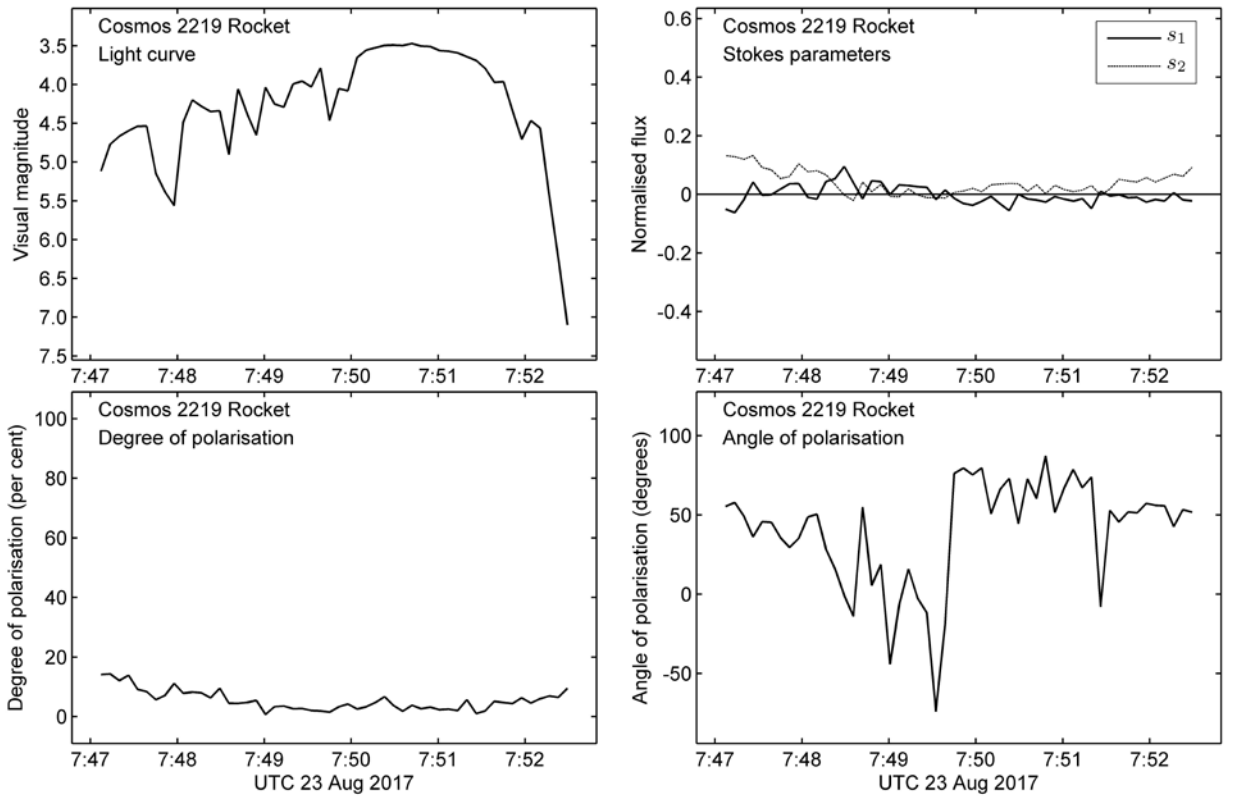

Fig. 11. Light curve and polarimetric signature of Cosmos 2219 Rocket (NORAD 22220).

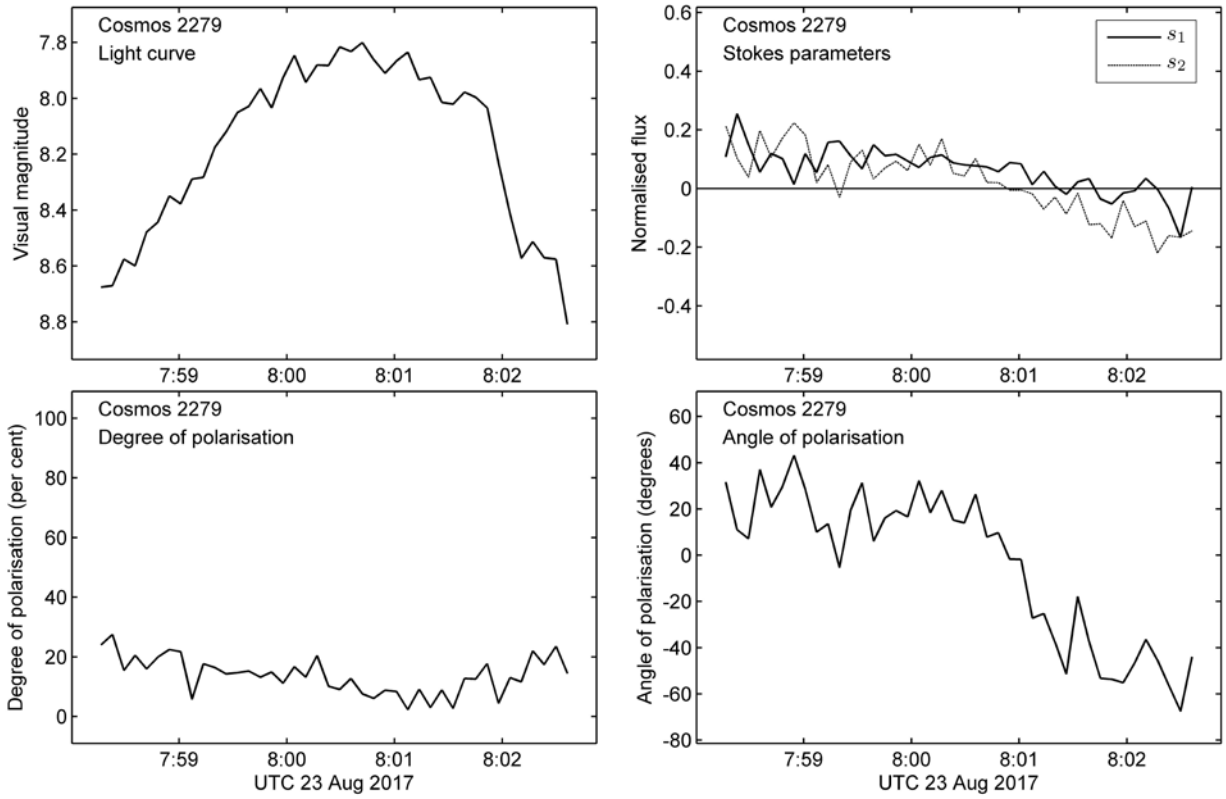

Fig. 12. Light curve and polarimetric signature of Cosmos 2279 (NORAD 23092).

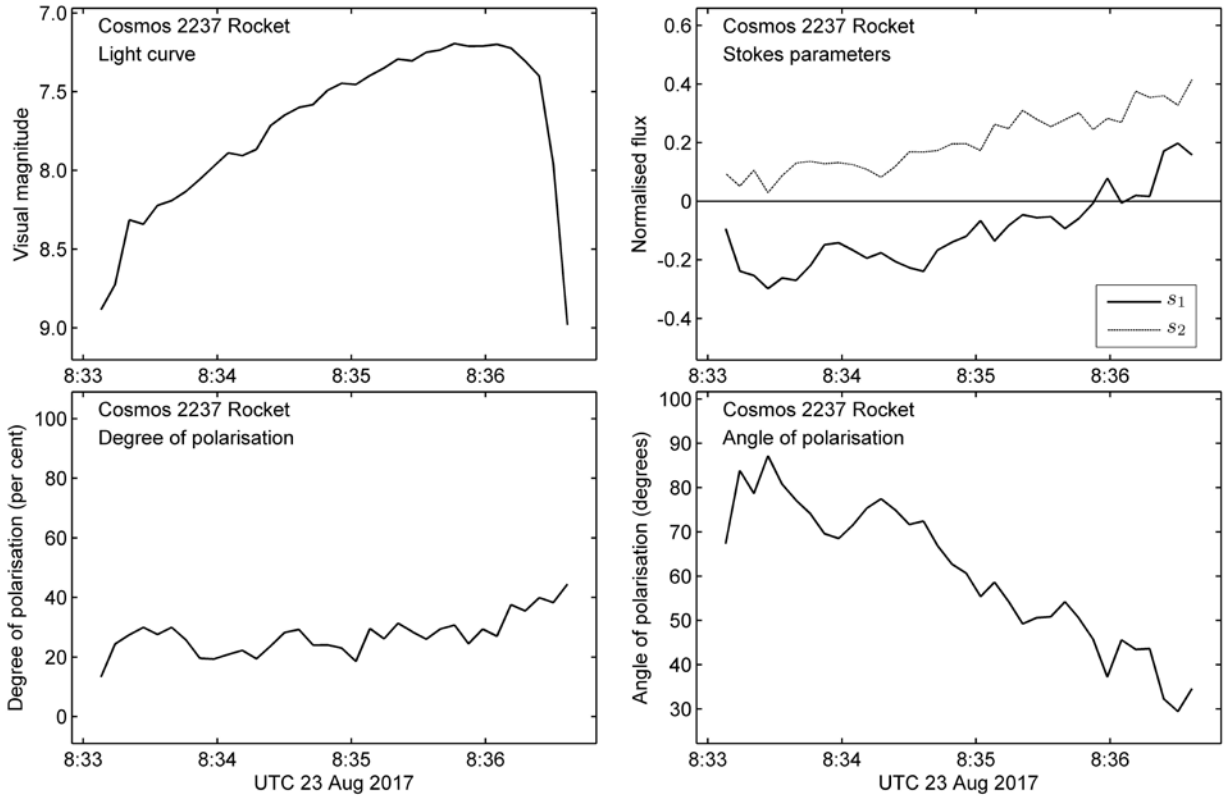

Fig. 13. Light curve and polarimetric signature of Cosmos 2237 Rocket (NORAD 22566).

6. SUMMARY

A number of satellites were observed from Whangaparaoa Peninsula, just north of Auckland, New Zealand, using the new quadruple polarimetric camera (QuadCam) built at the Defence Technology Agency as a result of collaboration with the Defence Science and Technology Laboratory, United Kingdom. Some modifications were made to the original UK design in order to improve the performance. The camera records a satellite in four polarisation planes simultaneously, which enables the calculation of the polarimetric signature in terms of Stokes parameters, as well as the degree and angle of polarisation. In addition, a specialised GPS timing unit attached to the camera records the time to accuracy better than 1 ms, which is essential for observations of satellites in low Earth orbit. The absolute detection limit after five seconds of exposure is about visual magnitude 10. It was demonstrated that relatively inexpensive equipment can be used for obtaining polarimetric signatures of satellites. The additional information derived from polarimetric data complements the standard photometric measurements and reveals some aspects related to the nature and behaviour of the satellite. This can be used for characterisation of unresolved objects in situations where high-resolution imaging is not available. Additional theoretical modelling is required to properly interpret the polarimetric signatures.

7. REFERENCES

1. Skuljan, J. and Kay, J., Automated astrometric analysis of satellite observations using wide-field imaging, Proc. 17th AMOS Conf., 2016, 240-249
2. Privett, G.J., Ashe, M.D., Greaves, M.J., Holland, D., Davidson, L., Polarimetric imaging for air-accident investigation, Proc. SPIE 8541, Electro-Optical and Infrared Systems: Technology and Applications IX, 2012.
3. Polo, M.C., Alenin, A., Vaughn, I., Lambert, A., GEO satellite characterization through polarimetry using simultaneous observations from nearby optical sensors, Proc. 17th AMOS Conf., 2016, 209-219
4. Collett, E., Field Guide to Polarization, SPIE Press, 2005
5. Hecht, E., Optics, 3rd edition, Addison Wesley Longman, 1998
6. Karttunen, H., Kröger, P., Oja, H., Poutanen, M., Donner, K.J. (Eds.), Fundamental Astronomy, 6th edition, Springer, 2017.
7. Heavens-Above (online data). Retrieved from: http://www.heavens-above.com/
8. CelesTrak Satellite Catalog (SATCAT) Search (online data). Retrieved from: https://celestrak.com/satcat/search.asp
9. Space-Track Two-Line Elements (online data). Retrieved from: https://www.space-track.org